Mineralogy and Petrology (1995) 52: 113–126

Mineralogy and Petrology

Crystal chemistry and optics of bazzite from Furkabasistunnel (Switzerland)

Th. Armbruster[1], E. Libowitzky[2], L. Diamond[3], M. Auernhammer[2], P. Bauerhansl[2], Ch. Hoffmann[2], E. Irran[2], A. Kurka[2], and H. Rosenstingl[2]

[1] Laboratorium für chemische und mineralogische Kristallographie, Universität Bern, Switzerland
[2] Institut für Mineralogie und Kristallographie, Universität Wien, Austria
[3] Mineralogisches Institut, Universität Bern, Switzerland

With 4 Figures

Received June 21, 1993;
accepted October 19, 1993

Summary

The crystal structure of blue bazzite (space group P6/mcc, Z = 2, a = 9.501(1), c = 9.178(1) Å) with the composition $Be_3(Sc_{1.25}Fe^{3+}_{0.43}Mg_{0.32}Mn_{0.03}Al_{0.02})_{\Sigma=2.05} \cdot Si_6O_{18}[Na_{0.32}(n\ H_2O)]$ was refined from X-ray single-crystal data with 422 unique reflections to R = 2.2%. The structure is of the beryl type with octahedra strongly compressed parallel to the c-axis. The octahedral Me–O distance in bazzite is 2.080 Å compared to 1.904 Å in beryl. The flattening of octahedra leads to a larger a cell dimension in bazzite compared to beryl (9.209 Å). Two-valent cations (mainly Mg) in octahedral coordination are charge balanced by Na at (0, 0, 0) in the structural channels. Polarized single-crystal IR-spectra recorded between 400 and 8000 cm^{-1} indicate that H_2O in the structural channels is oriented with the H–H vector perpendicular to the c-axis. The IR-spectra show more absorption bands than known for type II H_2O in beryl thus the existence of more than one H_2O species or even OH-groups is very likely.

Refractive indices of the same bazzite were measured using a spindle-stage and employing the wavelength-temperature variation method yielding n_o = 1.6279(3), n_e = 1.6066(5) for 589 nm at 25 °C. The birefringence Δ = 0.0213 is significantly larger than the one of near end-member beryl (Δ = 0.0047). This high birefringence of bazzite is related to the electronic polarizability of octahedral Sc and Fe which increase n_o at a stronger rate than n_e. Transition metals in bazzite are also responsible for a higher refractive index dispersion than found for beryl.

Zusammenfassung

Kristallchemie und optische Eigenschaften des Bazzits aus dem Furkabasistunnel (Schweiz)

Die Kristallstruktur eines blauen Bazzits (Raumgruppe P6/mcc, Z = 2, a = 9.501(1), c = 9.178(1) Å) mit der Zusammensetzung $Be_3(Sc_{1.25}Fe^{3+}_{0.43}Mg_{0.32}Mn_{0.03}Al_{0.02})_{\Sigma=2.05} \cdot Si_6O_{18}[Na_{0.32}(n\ H_2O)]$ wurde von Röntgeneinkristalldaten mit 422 Reflexen zu R = 2.2% verfeinert. Die Struktur ist die des Berylltyps mit der Besonderheit, daß die Oktaeder entlang der c-Achse stark zusammengedrückt sind. Die oktaedrischen Me–O Abstände im Bazzit betragen 2.080 Å, im Gegensatz zu 1.904 Å im Beryll. Die Stauchung der Oktaeder im Bazzit führt zu einer längeren a-Achse als im Beryll (9.209 Å). Zweiwertige Kationen (vor allem Mg) in oktaedrischer Koordination werden durch Na auf (0, 0, 0), in den strukturellen Kanälen, neutralisiert. Polarisierte Einkristall-IR-Spektren zwischen 400 und 8000 cm^{-1} zeigen, daß H_2O Moleküle in den strukturellen Kanälen mit dem H–H Vektor senkrecht zur c-Achse orientiert sind. Die IR-Spektren weisen außerdem mehr Absorptionsbanden auf, als für den H_2O Typ II bekannt sind, sodaß entweder mehr als eine H_2O Spezies oder sogar OH-Gruppen sehr wahrscheinlich sind.

Brechungsindizes am gleichen Bazzit wurden auf einem Spindeltisch mit der Wellenlängen-Temperatur Variationsmethode gemessen und ergaben n_o = 1.6279(3), n_e = 1.6066(5) bei 589 nm und 25 °C. Die Doppelbrechung Δ = 0.0210 ist deutlich höher als für einen nahezu Endgliedberyll (Δ = 0.0047). Diese hohe Doppelbrechung des Bazzits wird durch die elektronische Polarisierbarkeit von oktaedrischem Sc und Fe verursacht, die n_o stärker ansteigen läßt als n_e. Übergangselemente im Bazzit sind auch für die höhere Dispersion der Brechungsindizes als im Beryll verantwortlich.

Introduction

Bazzite was first described from Baveno, Italy, by *Artini* (1915) as a scandium silicate of unknown formula. *Bergerhoff* and *Nowacki* (1955) and *Peyronel* (1956) solved the structure of bazzite from *Val Strem* (Tavetsch, Grissona, Switzerland) and from Baveno, respectively, and showed that bazzite is the Sc analogue of beryl. The first quantitative electron microprobe analysis $Be_3(Sc_{1.3}F_{0.6}Al_{0.1})Si_6O_{18}$ was reported by *Nowacki* and *Phan* (1964) for the Swiss bazzite. *Chistyakova* et al. (1966) describe a bazzite occurrence in Central Kazakhstan and give the formula $Be_{3.06} \cdot (Sc_{1.26}Fe_{0.17}Al_{0.03})\ (Fe_{0.31}{}^{2+}Mn_{0.13}Mg_{0.12})\ (Si_{5.93}Be_{0.07})O_{18} \cdot [Na_{0.55}K_{0.03}Cs_{0.01},\ 0.87\ H_2O]$. *Hänni* (1980) studied beryls and bazzites from alpine fissures. His analyses indicate that the octahedral position in bazzite is to ca. 50% occupied by Sc with additional $Fe^{2+,3+}$, and Mg but with only low Al occupancies (less than 10%). On the other hand, beryls from alpine fissures are rich in octahedral Al and contain only traces of Sc (up to 0.6 wt. % Sc_2O_3). *Hänni* (1980) assumed on the basis of his analyses that there might be a gap in the solid solution between beryl and bazzite. In addition, all alpine bazzites contain high amounts of divalent cations (Mg, Fe) in octahedral coordination. Charge balance is obtained by 0.4–0.6 Na per formula unit (pfu), assumed to occupy the structural channels. Fine grained $Be_3Sc_2Si_6O_{18}$ (a = 9.56, c = 9.16 Å) was synthesized by *Frondel* and *Ito* (1968) at 450 °C and 2 kbar. At higher temperatures mainly phenacite formed. The same authors also substituted Sc by Fe^{3+}, Cr^{3+}, V^{3+}, and Mn^{3+} and observed that the solid solution is extensive but does not extent to the Sc-free end-member. *Frondel* and *Ito* (1968) also report that the thermal stability of bazzite increases to higher temperature in the presence of Na. Unfortunately, chemical analyses of their

run products were not performed. Single-crystal Raman spectra of a small bazzite crystal from Furkabasistunnel (Switzerland) were reported by *Hagemann* et al. (1990). They observed a strong Raman band at 3594 cm^{-1} which agrees with type II H_2O in beryl described by *Wood* and *Nassau* (1967) from polarized IR spectra of beryl. Type II H_2O is associated to alkali ions nearby and has the H–H vector perpendicular to the *c*-axis. This also agrees with the Na-rich electron microprobe analysis of bazzite from Furkabasistunnel, for which *Hänni* (1980) reported the composition range $Be_3(Sc_{1.13}Fe_{0.48}Me_{0.37}Mn_{0.02}Al_{0.09})Si_{6.04}O_{18}[Na_{0.40}Ca_{0.03}]$ to $Be_3(Sc_{0.97}Fe_{0.57}Mg_{0.40}Mn_{0.02}Al_{0.20})Si_{6.02}O_{18}[Na_{0.39}Ca_{0.04}]$. A single crystal from the same hand specimen as used by *Hänni* (1980) and *Hagemann* et al. (1990) was also used in this study. The locality of this sample was reported by *Stalder* (1978). The aim of the present study is to investigate the influence of Sc substitution in beryl on structural distortions and optical properties.

Experimental procedures

Electron microprobe analyses

Analyses were performed on a CAMECA SX50 electron microprobe using a 15 kV, 20 nA beam and conventional wave-length-dispersive crystal spectrometers equipped with gas-flow proportional detectors. Sc Kα-emission was calibrated with synthetic Sc_2TiO_5. Si, Al, K, Na, and Ca were calibrated on natural feldspars and Fe, Ti, Mn, and Cr were calibrated on synthetic oxides. The acquired signals were corrected for atomic number, absorption and secondary fluorescence effects by a standard PAP procedure (*Pouchou* and *Pichoir*, 1984). Results for the same bazzite crystal (NMBE-B440) as used for structure refinement and for a golden-yellow beryl from Brazil are given in Table 1.

X-ray measurements

A blue NMBE-B440 Furkabasistunnel bazzite crystal was mounted on a CAD4 single-crystal diffractometer with graphite monochromatized MoKα-radiation. Cell dimensions were refined from reflections with $30° > \Theta > 20°$ in hexagonal symmetry yielding $a = 9.501(1)$, $c = 9.178(1)$ Å, $V = 717.5(1)$ Å^3. In spite of the sharp optical extinction under crossed polarizers, the crystal displayed strongly smeared reflections parallel to the Ω direction indicating a strong mosaic pattern. Crystals from other occurrences: *Kentsk* (Kazakhstan), *Val Stream* (Switzerland), *Stremhörner* (Switzerland), *Fibbia, Gotthard* (Switzerland) were previously excluded because they showed strong alterations, inclusions or other inhomogeneities. Although the reflections were streaked, the Furkabasistunnel bazzite showed the best crystal quality of all bazzites checked with a polarizing microscope. A routine single crystal data set was collected up to 40 °Θ with $h < 18$, $k < 18$, $l < 17$ in a 4 °Ω scan mode comprising 1753 reflections. Data reduction, including background and Lorentz-polarisation corrections, was carried out using the SDP (*Enraf Nonius*, 1983) program library. The program SHELX76 (*Sheldrick*, 1976) was used for structure refinement. In order to obtain reliable occupancies with associated standard deviations for channel positions the refinement was carried out on the basis

Table 1. *Electron microprobe analyses of bazzite from Furka-basistunnel and golden-yellow beryl from Brazil*

Oxide	Bazzite wt %	Beryl wt %
SiO_2	59.79	66.27
Al_2O_3	0.17	17.81
Sc_2O_3	14.28	0.00
BeO*	12.5	13.8
MgO	2.11	0.66
Fe_2O_3	5.68	0.56
MnO	0.33	0.03
CaO	0.05	0.00
Na_2O	1.62	0.57
K_2O	0.00	0.04
Sum	96.54	99.74

* BeO calculated to yield 3 Be per formula unit

Number of cations on the basis of six Si

Si	6.0	6.0
Al	0.02	1.90
Sc	1.25	0.00
Be	3.01	3.00
Mg	0.32	0.09
Fe^{3+}	0.43	0.04
Mn^{2+}	0.03	0.00
Ca	0.00	0.00
Na	0.32	0.10
K	0.00	0.01

of 422 unique reflections with $\sin\Theta/\lambda > 0.4$ and $I > 3\sigma(I)$ using a $1/\sigma^2$ weighting scheme (space group P6/mcc). An extinction and absorption correction was applied. The agreement factor on symmetry related reflections was 1.4% based on F_{obs}. Neutral-atom scattering factors and real as well imaginary anomalous dispersion corrections were used. According to our electron microprobe analysis, the octahedral site was constrained to be occupied by 62.5% Sc. Mg and Fe were allowed to vary in order to fill this octahedral position. Oxygen, representing channel H_2O, was assigned to (0, 0, 1/4) and channel Na to (0, 0, 0). Both channel occupancies were refined. Because a Be analysis was not available for bazzite, the Be occupancy was allowed to vary in an additional test refinement. All atoms were refined with anisotropic displacement parameters. Coordinates, occupancies, and displacement parameters are given in Table 2. The refinement converged to $R = 2.2\%$, $R_w = 2.2\%$

Table 2. *Positional parameters, $B_{eq}[Å^2]$, and anisotropic displacement parameters with standard deviations in parentheses of bazzite from Furkabasistunnel*

Site	x/a	y/b	z/c	B_{eq}
A	2/3	1/3	1/4	0.675(8)
Si	0.37572(4)	0.10079(4)	0	0.547(6)
Be	1/2	1/2	1/4	0.71(2)
O1	0.3002(2)	0.2198(1)	0	1.01(1)
O2	0.4835(1)	0.1304(1)	0.14454(8)	0.87(1)
W	0	0	1/4	2.9(2)
Na	0	0	0	1.3(1)

Occupancies: A: 0.62 Sc, 0.23(2) Fe, 0.15(2) Mg; W: 0.8(1) O; Na: 0.46(4) Na
Note: $B_{eq} = 8/3\ \pi^2\Sigma_i(\Sigma_j[U_{ij}a_i{*}a_j{*}a_ia_j])$

Site	U_{11}	U_{22}	U_{33}	U_{12}	U_{13}	U_{23}
A	0.0086(3)	0.0086(3)	0.0084(3)	0.0043(1)	0	0
Si	0.0075(2)	0.0069(2)	0.0065(2)	0.0038(1)	0	0
Be	0.0106(6)	0.0106(6)	0.0066(7)	0.0059(7)	0	0
O1	0.0143(4)	0.0112(4)	0.0166(4)	0.0091(3)	0	0
O2	0.0133(3)	0.0111(3)	0.0090(3)	0.0063(2)	−0.0039(2)	−0.0011(2)
W	0.043(5)	0.043(5)	0.022(5)	0.022(3)	0	0
Na	0.010(2)	0.010(2)	0.030(3)	0.005(1)	0	0

Note: displacement parameters are of the form: $\exp[-2\pi^2(U_{11}h^2a^{*2} + U_{22}k^2b^{*2} + U_{33}l^2c^{*2} + 2U_{12}hka^*b^* + 2U_{13}hla^*c^* + 2U_{23}klb^*c^*)]$

with 35 parameters. The largest residual peaks in difference Fourier maps were ± 0.3 e/Å^3.

IR spectroscopy

Polarized infrared spectra of four well developed hexagonal prismatic bazzite crystals from Furkabasistunnel (NMBE-B440) with a size between 0.12 × 0.12 × 0.5 mm and 0.25 × 0.25 × 2 mm were recorded on an PERKIN ELMER 1760X FT-IR spectrometer equipped with a FT-IR microscope. Objective and condenser cassegrains with a numerical aperture of 0.60 were used. The measuring spot was limited to 0.1 mm by a field aperture. The spectra were recorded through the shiny parallel prism faces after spreading the crystals on a MgF_2 window. Thus the crystals were investigated without any previous preparation like grinding or polishing. Polarized spectra were collected parallel and perpendicular to the *c*-axis in the region between 400 and 8000 cm^{-1} at a resolution of 4 cm^{-1} (Fig. 1). Each of the spectra was averaged from 100 single measurements to minimize background noise. According to the sample thickness of 0.12 to 0.25 mm, the average transmission rate varied between 15 and 28%. Consequently, some very strong absorptions were cut by the baseline at about 0% transmission.

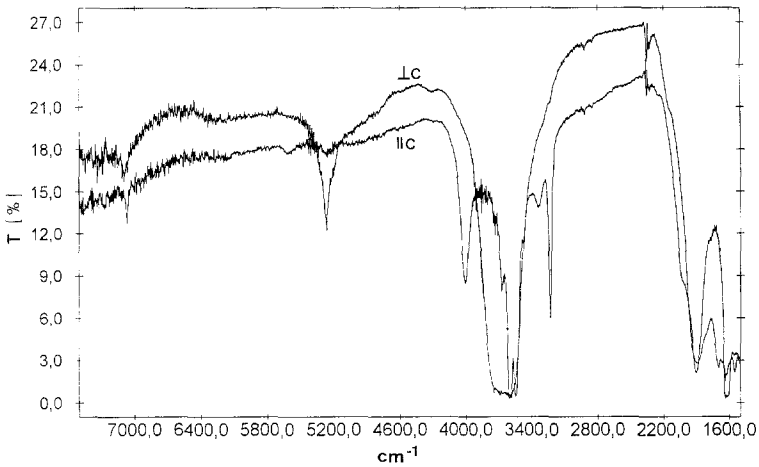

Fig. 1. Polarized single crystal IR spectra of bazzite from Furkabasistunnel. Observed absorption bands are summarized in Table 6

Table 3. *Refractive indices at 589.3 nm, 25 °C*

	X	Z	Δ
Bazzite (1)	1.6279(3)	1.6066(5)	0.0213
Beryl (2)	1.5725(2)	1.5678(2)	0.0047
Beryl nat (3)	1.5741(3)	1.5695(5)	0.0046
Beryl heated (3)	1.5645(5)	1.5606(3)	0.0039

(1) Furkabasistunnel
(2) Siberia (*Isetti*, 1961)
(3) Brazil (Table 1)

Crystal optics

Optical properties of the same bazzite crystal as used for electron microprobe analysis and structure refinement were determined with a polarizing microscope equipped with a spindle stage. The crystal orientation was derived from the distinct hexagonal prismatic morphology 0.14 × 0.14 × 0.70 mm. The crystal was pleochroic: light blue parallel *c*, light yellow parallel *a*. The λ – T double-variation method (*Bloss*, 1981) was applied using calibrated Cargille immersion liquids. Refractive indices were measured between 450 and 650 nm at 22–35 °C using the Becke-line technique. The dispersion of refractive indices was refined from λ – T data according to the Cauchy and Sellmeier equations using the program SOLID (*Su* et al., 1987; *Gunter* et al., 1989). In addition, the same procedure was used to measure optical properties of a light yellow almost end-member beryl from Brazil (Table 1), $Be_3Al_{1.90}Fe_{0.04}Mg_{0.09}Si_6O_{18}[Na_{0.10}(n \cdot H_2O)]$, in its natural state ($a$ = 9.208(1), c = 9.188(2) Å) and after dehydration for 12 h at 950 °C (a = 9.210(2), c = 9.190(1) Å). The *c*-axis dimension of 9.19 Å also indicates (*Bakakin* et al., 1970) that only very minor Li substitutions for Be must be considered. The decrease of refractive indices upon heating to 950 °C can be related to the loss of volatiles (mainly water) from the structural channels.

Table 4. *Sellmeier dispersion constants for bazzite and beryl*

	Bazzite X	Beryl (1) X	Beryl nat X	Beryl heat. X
a_0	0.6273(3)	0.6970(3)	0.6937(5)	0.7083(9)
a_1	−7736(69)	−6244	−5873(144)	−6060(264)
λ_0 [nm]	108.1	94.6	92.0	92.5
E_0 [eV]	11.5	13.1	13.5	13.4
	Bazzite Z	**Beryl (1) Z**	**Beryl nat Z**	**Beryl heat. Z**
a_0	0.6524(6)	0.7043(2)	0.7027(8)	0.7160(4)
a_1	−7046(172)	−6343	−6551(224)	−6722(131)
λ_0 [nm]	103.9	94.9	96.6	96.9
E_0 [eV]	11.9	13.1	12.8	12.8

(1) Siberia (*Isetti*, 1961)

Isetti (1961) reported dispersion data between 460 and 700 nm of a pale green beryl from Siberia measured with the minimum deviation method using cut crystal prisms. Cell dimensions or a chemical composition of the Siberian sample are not given. However, refractive indices indicate low alkali and transition metal concentrations (*Černy* and *Hawthorne*, 1976). *Isetti's* (1961) measurements were also submitted to a linearized single-term Sellmeier equation (e.g. *Bloss*, 1981): $y = a_0 + a_1 x$, where y represents $(n^2 - 1)^{-1}$, a_0 represents A^{-1} (A is proportional to the strength of the absorption band at λ_0), a_1 represents $(-\lambda_0^2/A)$, and x represents λ^{-2}. Resulting refractive indices of beryls and bazzite with corresponding dispersion constants are summarized in Tables 3 and 4.

Results

Crystal structure

The refined formula for Furkabasistunnel bazzite is $Be_3(Sc_{1.25}Fe_{0.46(4)}Mg_{0.29(4)}) \cdot Si_6O_{12}[Na_{0.46(4)} \cdot (H_2O)_{0.8(1)}]$. We have to keep in mind, that in the structure refinement low concentrations of octahedral Al are modelled by Mg and octahedral Mn by Fe because of the similarity in corresponding scattering factors. Thus the refined octahedral occupations are in good agreement (within 3 e.s.d's) with the composition analyzed on the surface of the bazzite prism face (Table 1). The refined Na concentration (0.46 Na pfu) on (0, 0, 0) is slightly higher than the analytically determined amount of Na + Ca which should yield Na occupancies of 0.32 pfu. It could be speculated that either additional H_2O or low concentrations of heavy elements also occupy this channel site at (0, 0, 0). For crystals from the same hand specimen *Hänni* (1980) analyzed sums of Al + Sc + Fe + Mn + Mg which ranged between 2.10 and 2.16. Our own analysis gave a value of 2.05 indicating that some of these cations may occur on channel sites. The assumption of transition metals in the structural channels is also confirmed by various spectroscopic studies on Fe-bearing beryls (e.g. *Goldman* et al., 1978; *Blak* et al., 1982; *Smith* et al., 1976). Test

Table 5. *Interatomic distances [Å] and angles [°] for Furkabasistunnel bazzite compared with beryl (Morosin, 1972) in italics*

SiO_4 tetrahedron		
Si–O1	1.616(1)	*1.592(1)*
Si–O1	1.613(1)	*1.594(1)*
Si–O2 (2x)	1.612(1)	*1.620(1)*
O1–O1	2.558(1)	*2.582(1)*
O2–O1 (2x)	2.645(1)	*2.607(1)*
O2–O1 (2x)	2.650(1)	*2.638(1)*
O2–O2	2.652(1)	*2.668(1)*
O1–Si–O1	104.81(5)	*108.24(3)*
O2–Si–O1 (2x)	110.52(4)	*108.42(2)*
O2–Si–O1 (2x)	110.08(3)	*110.40(2)*
O2–Si–O2	110.68(3)	*110.88(2)*
Si–O1–Si	164.81(7)	*168.24(3)*
BeO_4 tetrahedron		
Be–O2 (4x)	1.642(1)	*1.653(1)*
O2–O2 (2x)	2.483(1)	*2.355(1)*
O2–O2 (2x)	2.650(1)	*2.688(1)*
O2–O2 (2x)	2.893(1)	*3.012(1)*
O2–Be–O2 (2x)	98.28(3)	*90.90(2)*
O2–Be–O2 (2x)	123.45(4)	*131.40(2)*
O2–Be–O2 (2x)	107.66(4)	*108.85(2)*
Si–O2–Be	130.20(5)	*127.05(2)*
AO_6 octahedron		
A–O2 (6x)	2.080(1)	*1.904(1)*
O2–O2 (3x)	2.483(1)	*2.355(1)*
O2–O2 (3x)	2.868(1)	*2.712(1)*
O2–O2 (6x)	3.188(1)	*2.847(1)*
O2–A–O2 (3x)	73.29(3)	*76.40(1)*
O2–A–O2 (3x)	87.15(3)	*90.79(1)*
O2–A–O2 (6x)	100.06(3)	*96.76(1)*
O2–A–O2 (3x)	171.07(3)	*170.40(1)*
Structural channel		
Na–O1 (6x)	2.558(1)	
Na–W (2x)	2.295	

refinements indicated that the Be site is completely occupied by Be. Interatomic distances and angles are given in Table 5.

IR spectroscopy

The resulting polarized infrared spectra showed identical absorption bands for all four bazzite crystals. The absorption bands and approximate intensities with polarization parallel and perpendicular to the *c*-axis are listed in Table 6.

Table 6. *Infrared absorptions of H_2O in bazzite*

Frequency [cm^{-1}]	Perpendicular to *c*	Parallel to *c*	Assignment
7070	—	very weak	$2\nu_1$ H_2O type II
7100	very weak	—	$\nu_1\nu_3$ H_2O type II
5262	strong	—	$\nu_2\nu_3$ H_2O type II
4003	weak shoulder	strong	?
3735	—	very weak	?
3670	—	very weak	?
3650	very strong, broad	—	ν_3 H_2O type II
3593	—	strong	ν_1 H_2O type II
3542	—	strong	?
3475	—	very weak	?
3330	—	weak	?
3270	strong shoulder	—	?
3227.5	—	strong	$2\nu_2$ H_2O type II
1625	—	medium	ν_2 H_2O type I

Note: band assignments according to *Wood* and *Nassau* (1967) and *Herzberg* (1960)

Infrared spectra of these bazzite crystals show evidence for type II H_2O but not for type I H_2O which has the H–H vector parallel to the *c*-axis. There is also no CO_2 within the structural channels with an absorption band at about 2354 m^{-1} (*Wood* and *Nassau*, 1967; *Aines* and *Rossman*, 1984). In addition to the type II H_2O bands there are several polarized bands related to H_2O or OH groups.

Optics

Table 3 indicates that Furkabasistunnel bazzite and near end-member beryl can easily be distinguished on the basis of their refractive indices and birefringence which are significantly higher for bazzite. A blue sodic beryl with high Fe and Mg content $(Al_{1.26}Fe^{3+}_{0.15}Fe^{2+}_{0.16}Mg_{0.42})Be_{2.94}Si_{6.07}O_{18}[Na_{0.45}(H_2O)_{0.95}]$ which resembles macroscopically bazzite due to a similar color and pleochroism has $n_o = 1.603$, $n_e = 1.595$ (*Sanders* and *Doff*, 1991) and a synthetic (hydrothermal) almost Fe-end member beryl $Al_{0.07}Fe_{1.87}Mg_{0.06}Mn_{0.02}Be_3Si_{6.09}O_{18}[Na_{0.49}(H_2O)_x]$ has $n_o = 1.659$ and $n_e = 1.640$ ($a = 9.435$, $c = 9.163$ Å; *Hänni*, 1980). Thus the question arises whether bazzites can also be distinguished by their refractive indices from sodian Fe-bearing beryls which show macroscopically the same morphology and blue color. To obtain a beryl data set comparable to bazzite, we considered only beryls of the octahedral substitution type with 0.33 pfu < Na < 0.46 pfu from the data of *Hänni* (1980) and *Aurisicchio* et al. (1988). These beryls have 0.19 pfu < Mg < 0.46 pfu, or in other words, divalent Mg replacing trivalent Al is the major cause for Na in the structural channels. Excess Na is mainly balanced by octahedral ferrous iron. From the data of *Hawthorne* and *Černy* (1977) and *Sherriff* et al. (1991) we further assume that each Na is bonded to 2 H_2O. The average chemical formula of a corresponding beryl solid solution series is $(Al_{1.6-x}Mg_{0.4}(Fe, Mn, Cr)_x)Be_3Si_6O_{18}$.

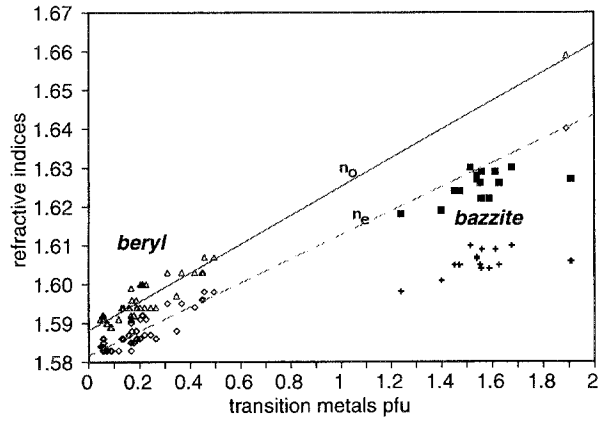

Fig. 2. The concentration of transition elements per formula unit (pfu) in beryls with the simplified composition $(Al_{1.6-x}Mg_{0.4}(Fe, Mn, Cr)_x)Be_3Si_6O_{18}[Na_{0.4}(H_2O)_{0.8}]$ and of bazzites with the simplified composition $((Sc, Fe, Mn)_{2-x}Mg_x)Be_3Si_6O_{18}[Na_{0.45}(H_2O)_{0.9}]$ is plotted versus refractive indices (n_o, n_e). Beryls describe a linear trend, whereas bazzites do not obey this correlation but show a strong birefringence and plot below the beryl curves. Data from *Hänni* (1980) and *Aurisicchio* et al. (1988)

$[Na_{0.4}(H_2O)_{0.8}]$. For these data refractive indices are plotted versus the concentration of transition metals per formula unit. A linear regression analyses including a synthetic sodian iron-beryl (*Hänni*, 1980) yielded the lines shown in Fig. 2. Bazzites retrieved from the data of *Hänni* (1980) can be written with the average formula $((Sc, Fe, Mn)_{2-x}Mg_x)Be_3Si_6O_{18}[Na_{0.45}(H_2O)_{0.9}]$. Refractive indices of these bazzites are also plotted in Fig. 2 and describe a different trend. The reason why refractive indices of bazzites plot below the beryl curve can be explained by the larger cell volume and the smaller density of bazzites compared to Fe, Mg-rich beryls with the same transition metal concentration.

It is well known (e.g. *Strens* and *Freer*, 1978) that a high content of transition metals in a mineral structure shifts the UV absorptions to higher wavelengths. This can be calculated from refractive index dispersion data using the single absorption band model of the Sellmeier equation (e.g. *Bloss*, 1981, *Armbruster*, 1985). Following this model, a shift of UV absorptions (λ_0) towards higher wave lengths is accompanied with an increase of refractive index dispersion (Table 4). Bazzite yields λ_0 values between 104 and 108 nm whereas the absorption wave lengths between 92 and 97 nm were calculated for beryl. The reciprocal of a_0 is proportional to the strength of the absorption band which is stronger for bazzite than for beryl.

Discussion

The structure refinement of Furkabasistunnel bazzite agrees well with observations made on beryl (e.g. *Morosin*, 1972; *Aurisicchio* et al., 1988; *Sanders* and *Doff*, 1991). In Na-rich beryls (*Sanders* and *Doff*, 1991) and bazzites, Na occupies the center of the six-membered rings thus the coordination and the bond valence of O1 increases, which in turn leads to a lengthening of Si–O1 distances compared to end-member beryl (Table 5). Simultaneously, Si–O2 distances in Na-rich samples shorten in order to satisfy Si^{4+} bond valence requirements (Table 5). Be–O2 distances in bazzite are

slightly shorter than in end-member beryl but the BeO_4 tetrahedra in bazzite are less distorted (Table 5). Octahedra in bazzite are strongly compressed along *c* yielding a separation of the adjacent triangular faces parallel to (001) of 2.651 Å, whereas 2.670 Å are calculated for Al octahedra in beryl (*Morosin*, 1972). This indicates that in spite of the larger Me–O2 distances in bazzite (2.080 Å) compared to Al–O2 distances in beryl (1.904 Å), bazzite octahedra are strongly flattened and angularly distorted. This octahedral flattening is also responsible for the larger *a* cell dimension (9.501 Å) in bazzite compared to 9.209 Å in beryl. The Na–H_2O distance in bazzite and sodian beryl (*Sanders* and *Doff*, 1991; *Aurisicchio* et al., 1988) is surprisingly short (2.295 Å in bazzite). Anisotropic displacement parameters for Na and H_2O are quite high thus it must be assumed that Na is slightly shifted out of the plane defined by the six-membered rings. H_2O strongly vibrates perpendicular to the *c*-axis. These arguments, however, must be exercised with caution because, as shown above, additional cations may occupy the channel site at (0, 0, 0). Bazzite from Furkabasistunnel represents a strongly disordered structure because cations with a large range of ionic radii (Fe^{3+}: 0.645 Å, Sc: 0.745 Å; *Shannon*, 1976) occupy octahedral sites. In addition, approximately 40% of the six-membered rings are centered by cations, thus, as discussed before, Si–O distances vary depending on neighboring Na. These disorders give rise to large displacement parameters of all atoms in bazzite compared to end-member beryl (*Morosin*, 1972).

The polarized single-crystal IR spectra (Table 6) agree with those given by *Wood* and *Nassau* (1967) for type II H_2O in beryl. Absorptions assigned to type I H_2O (*Wood* and *Nassau*, 1967) were not found which is explained by the high channel cation concentration in the bazzite studied. The high channel cation concentration requires that H_2O must always be associated with cations.

Our IR spectra show many more absorptions than reported in previous studies for H_2O in beryl (*Wood* and *Nassau*, 1967; *Aines* and *Rossman*, 1984). Two reasons may account for this discrepancy. Either these additional absorption bands were hitherto overlooked because all beryls studied by polarized IR single-crystal spectroscopy revealed a mixture of H_2O type I and type II, and in addition, all previous spectra were recorded on considerably thinner samples thus these bands were perhaps not so obvious; or the additional bands are characteristic of this bazzite. The strong and very sharp band at 3227.5 cm^{-1} is not particularly described and explained by *Wood* and *Nassau* (1967) but in their spectra one can recognize humps at this frequency, growing in intensity for beryls with increasing alkali concentrations. A weak band at 7070 cm^{-1} may be explained by an overtone of ν_1 and the strong band at 3227.5 cm^{-1} by an overtone of ν_2. The additional bands at 4003, 3735, 3670, 3542, 3475, and 3330 cm^{-1} which were found in all crystals studied are probably related to H_2O and/or OH in a somewhat different coordination sphere.

The high birefringence of bazzite is related to the high electronic polarizability of mainly Sc which has its strongest effect perpendicular to the *c*-axis, thus increasing n_o to a higher rate than n_e. This effect is not compensated by expansion of the structure parallel to *a*.

Aurisicchio et al. (1988) observed a compositional gap between so called 'octahedral beryls' where Al is replaced by divalent metals and 'tetrahedral beryls' where Be is substituted by Li. The above authors speculate that opposite distortions with regard to the octahedron and tetrahedron may be the reason for the two distinct series. Our study on bazzite confirms this assumption which is also

supported by previous studies on double-ring silicates (*Armbruster* and *Oberhänsli*, 1988). Al is one of the smallest cations occurring in octahedral coordination. Substitution of Al in the beryl structure by other cations, independent of whether they are bivalent or three-valent, will increase the octahedral volume. The size of Al octahedra and Be tetrahedra in beryl are constrained to each other because they share two edges. The second constraint comes from the size and hexagonal symmetry of the Si_6O_{18} rings. If the octahedron expands the O2a–O2b distance forming an octahedral edge (Fig. 3) then the adjacent O2b–O2c distance, forming a BeO_4

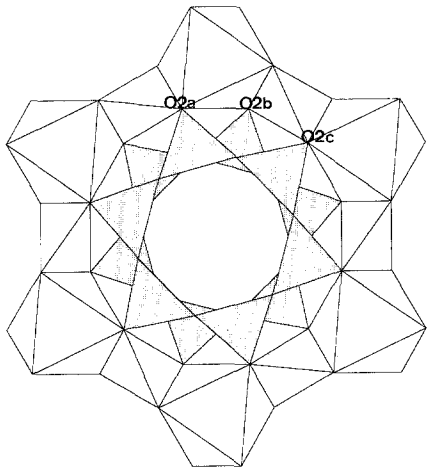

Fig. 3. View of the bazzite structure parallel to the *c*-axis. The twelve-membered ring of edge-sharing octahedra and tetrahedra is linked by O2 type oxygen to the six-membered rings of tetrahedra. The six-membered rings of tetrahedra constrain the size of octahedra and tetrahedra in the outer ring. The distance O2a–O2c is fixed in beryl structures where only Si occupies the six-membered rings of tetrahedra. Thus large octahedra lead to long O2a–O2b separation, forcing the O2b–O2c distance to be short and vice versa

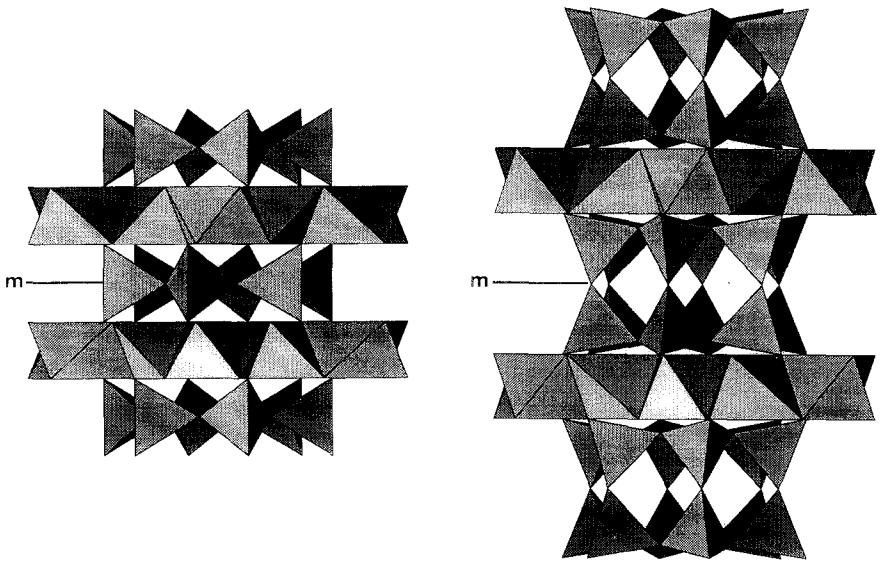

Fig. 4. Coordination polyhedra model of the beryl-type bazzite structure (left) and the double-ring silicate type structure of sugilite (right) viewed perpendicular to the *c*-axis. In the beryl structure, a mirror plane perpendicular to the *c*-axis forces one tetrahedral edge of the SiO_4-tetrahedra to run parallel to the *c*-axis. The structure of double-ring silicates has the mirror plane between two adjacent six-membered rings, allowing the SiO_4 tetrahedra to kink in a way that the outer tetrahedral edges are inclined to the *c*-axis. This variable kinking of the double-ring silicate units gives the structure more flexibility to adjust to various sizes of octahedra and tetrahedra in the edge-sharing twelve-membered rings

tetrahedral edge, has to be shortened and vice versa. This is confirmed for bazzite which has a larger octahedron but a more compressed tetrahedron than beryl (Table 5). Li replacing Be is significantly larger with an average tetrahedral Li–O distance of 1.96 Å (*Wenger* and *Armbruster*, 1991). Thus both substitution types, the 'tetrahedral series' and the 'octahedral series' lead to an increase of both, the tetrahedral and the octahedral volume which is incompatible with the relatively rigid size of the Si_6O_{18} rings. The same correlation was found in double ring silicates (*Armbruster* and *Oberhänsli*, 1988). The more extensive chemical variability of double-ring silicates contrasted by the beryl-type ring-silicates is mainly caused by a mirror-plane perpendicular to the c-axis which in double-ring silicates lies between two stacked six-membered rings (Fig. 4) whereas in the beryl structure the mirror plane intersects the Si_6O_{18} rings thus their upper and lower half become symmetry related. Therefore, double-ring units of tetrahedra are more flexible to adopt the size of surrounding cations. This is the reason why many minerals and synthetic compounds crystallize in the structure of the double-ring silicate type but only few are found with the beryl structure.

Acknowledgements

The optical studies in this paper were carried out during a course 'Spindle stage optics and optical properties of minerals' held by the senior author in spring 1993 at the University of Vienna. *B. Hofmann* (Museum of Natural History, Bern) kindly provided bazzite samples from the museum collection. Bazzite from Furkabasistunnel is deposited at the Museum of Natural History, Bern, under NMBE-B440. *A. Beran* (Vienna) kindly provided the IR equipment which is highly appreciated. We acknowledge support for the electron microprobe of the University of Bern by Schweizerischer Nationalfonds (Credit 21-26579.89).

References

Aines D, Rossman GR (1984) The high temperature behavior of water and carbon dioxide in cordierite and beryl. Am Mineral 69: 319–327

Armbruster Th (1985) Kristalloptik transparenter Minerale im sichtbaren Licht. Fortschr Mineral 63: 91–109

Armbruster Th, Oberhänsli R (1988) Crystal chemistry of double-ring silicates: structures of sugilite and brannockite. Am Mineral 73: 594–600

Artini E (1915) Due minerali di Baveno contenti terre rare: weibyite e bazzite. Rend Accad Lincei 24: 313–319

Aurisicchio C, Fioravanti G, Grubessi O, Zanazzi PF (1988) Reappraisal of the crystal chemistry of beryl. Am Mineral 73: 826–837

Bakakin VV, Rylov GM, Belov NV (1970) X-ray diffraction data for identification of beryl isomorphs. Geokhimiya 11: 1302–1311 [English translation in: Geochem Int (1970): 924–933]

Bergerhoff G, Nowacki W (1955) Ueber die Kristallstruktur des Bazzit und ihre Beziehungen zu der des Beryll. Schweiz Mineral Petrogr Mitt 35: 410–421

Blak AR, Isotani S, Watanabe S (1982) Optical absorption and electron spin resonance in blue and green beryl. Phys Chem Minerals 8: 161–166

Bloss FD (1981) The spindle stage: principles and practice. Cambridge University Press, Cambridge London New York New Rochelle Melbourne Sidney, p 340

Černy P, Hawthorne FC (1976) Refractive indices versus alkali content in beryl: general limitations and applications to some pegmatite types. Can Mineral 14: 491–497

Chistyakova MB, Movela VA, Rasmanova ZB (1966) The first find of bazzite in the USSR. Dokl Akad Nauk SSSR 169: 1421–1424

Enraf-Nonius (1983) Structure determination package (SDP). Enraf-Nonius, Delft, The Netherlands

Frondel C, Ito J (1968) Synthesis of the scandium analogue of beryl. Am Mineral 53: 943–953

Goldman DS, Rossman GR, Parkin KM (1978) Channel constituents in beryl. Phys Chem Minerals 3: 225–235

Gunter ME, Bloss FD, Su SHC (1989) Computer programs for the spindle stage and double variation method. Microscope 37: 167–171

Hagemann H, Lucken A, Bill H, Gysler-Sanz J, Stalder HA (1990) Polarized Raman spectra of beryl and bazzite. Phys Chem Minerals 17: 395–401

Hänni HA (1980) Mineralogische und mineralchemische Untersuchungen an Beryll aus alpinen Zerrklüften. Dissertation, Universität Basel

Hawthorne FC, Černy P (1977) The alkali-metal positions in Cs–Li beryl. Can Mineral 15: 414–421

Herzberg G (1960) Molecular spectra and molecular structure. II. Infrared and Raman spectra of polyatomic molecules. Van Nostrand, Princeton, pp 280–282

Isetti G (1961) Ricerche sulle relazioni esistenti tra birifrazione, dispersione e pleochroismo di alcuni minerali. Periodico di Mineralogia 30: 139–163

Morosin B (1972) Structure and thermal expansion of beryl. Acta Crystallogr B28: 1899–1903

Nowacki W, Phan KD (1964) Composition quantitative de la bazzite de Val Strem (Suisse) determine par la microsonde électronique de Castaigne. Bull Soc Mineral 87: 453

Peyronel G (1956) The crystal structure of Baveno bazzite. Acta Crystallogr 9: 181

Pouchou JL, Pichoir F (1984) Un nouveau modèle de calcul pour la microanalyse quantitative par spectrométrie de rayons X. La Recherche Aèrospatiale 3: 167–192

Sanders IS, Doff DH (1991) A blue sodic beryl from southeast Ireland. Min Mag 55: 167–172

Sheldrick GM (1976) SHELX76. Program for crystal structure determination. University of Cambridge, England

Shannon RD (1976) Revised effective ionic radii and systematic studies of interatomic distances in halides and chalcogenides. Acta Crystallogr A32: 751–767

Sherriff BL, Grundy HD, Hartman JS, Hawthorne FC, Černy P (1991) The incorporation of alkalis in beryl: multi-nuclear MAS NMR and crystal structure-study. Can Mineral 29: 271–285

Smith G, Dickson BL, Vance ER, Price, DC (1976) Optical and Mössbauer studies of beryl. 24th Intern Geol Congress, Sydney, Section 14, 602 (Abstract)

Stalder HA (1978) Alte und neue Mineralfunde aus dem Wallis. Schweizer Strahler 4: 374–384

Strens RG, Freer R (1978) The physical basis of mineral optics. I. Classical theory. Min Mag 42: 19–30

Su S-C, Bloss FD, Gunter ME (1987) Procedures and computer programs to refine the double-variation method. Am Mineral 72: 1011–1013

Wenger M, Armbruster Th (1991) Crystal chemistry of lithium: oxygen coordination and bonding. Eur J Mineral 3: 387–399

Wood DL, Nassau K (1967) Infrared spectra of foreign molecules in beryl. J Chem Phys 47: 2220–2228

Authors' addresses: *Th. Armbruster*, Laboratorium für chemische und mineralogische Kristallographie, Universität Bern, Freiestrasse 3, CH-3012 Bern, Switzerland; *L. Diamond*, Mineralogisches Institut, Universität Bern, Baltzerstrasse 1, CH-3012 Bern, Switzerland; *E. Libowitzky, M. Auernhammer, P. Bauerhansl, Ch. Hoffmann, E. Irran, A. Kurka*, and *H. Rosenstingl*, Institut für Mineralogie und Kristallographie, Universität Wien, Dr.-Karl-Lueger-Ring 1, A-1010 Wien, Austria